

Application of Electrical Resistivity and Chargeability Data on a GIS Platform in Delineating Auriferous Structures in a Deeply Weathered Lateritic Terrain, Eastern Cameroon

Albert Nih Fon^{1*}, Vivian Bih Che², Cheo Emmanuel Suh^{1,2}

¹Economic Geology Unit, Department of Geology, Faculty of Science, University of Buea, Buea, Cameroon

²Remote Sensing Unit, Department of Geology, Faculty of Science, University of Buea, Buea, Cameroon

Email: *fonberto2002@yahoo.com

Received July 24, 2012; revised August 27, 2012; accepted September 26, 2012

ABSTRACT

Exploration for primary gold in tropical settings is often problematic because of deep weathering and the development of a thick soil cover. In this paper we present the results of both chargeability and resistivity surveys carried out over the Belikombone hill gold prospect (14°00' - 14°25'E, 5°25' - 6°00'N) in the Betare Oya area (eastern Cameroon), where previous soil sampling had identified gold anomalies. The geophysical data were obtained using Syscal Junior 48 resistivity meter and the Schlumberger configuration array for both the vertical electrical soundings (VES) and horizontal profiling. These data were further built into a GIS framework and the continuity of favourable gold-bearing structures at depth modeled using WINSEV, RED2INV and SURFER extensions softwares. IP (Induced Polarization)-chargeability and resistivity data combined, have identified irregular anomalous zones trending NE-SW. This trend is consistent with the attitude of most auriferous quartz veins exposed in artisanal pits and parallel to the regional shear zone system and foliations. The high resistivity anomalies correspond to quartz veins while the relatively high IP anomalies correspond to low sulphide ± gold concentrations in the quartz veins. Modeling IP-chargeability and resistivity data prepared as contours and 3D maps, culminated to the development of an inferred, irregular and discontinuous mineralized body at depths of up to 95 m. The size and shape of this mineralized body can only later be tested by drilling to ascertain the resource.

Keywords: Gold Exploration; Tropical Settings; Deep Weathering; IP-Chargeability and Resistivity; Betare Oya; 3D Maps; Cameroon

1. Introduction

In many areas around the world, gold mineralization is structurally controlled [1-3] and usually associated with faults, fractures and shear zones. However, in humid tropical settings, where weathering processes are intense and the lateritic soil profiles deep, exploration efforts are hampered by the paucity of outcrops, vegetation cover and extensive alteration of truncated lateritic soil profiles. Recent alteration and reworking of the soil profile by surface processes, results in extensive modification and/or complete obliteration of previous primary geochemical dispersion patterns and pedological features of surface soils [4] further complicating the search for primary ore bodies at depth. For these reasons, soil geochemistry alone cannot be effectively used in locating deeply em-

bedded and hidden mineralized primary ore bodies (often referred to as blind ore bodies). Geochemical exploration in such areas therefore, is often supplemented by geophysical techniques including combined IP-chargeability and resistivity surveys. In the Belikombone hill investigated in this study, gold mineralization is associated with metallic sulfides and oxides, which are excellent electrical conductors, making it possible to target them using geoelectrical exploration methods.

Such ground geophysical surveys, in which the resistivity and chargeability of subsurface materials can be measured, is capable of delineating zones of high chargeability and low resistivity which may represent potential areas of mineralization. Geophysical techniques such as self potential (SP), gravity combined with induced polarization (IP) and resistivity techniques have been used in the investigation of huge hydrothermal systems, active volcanoes and large geological structures

*Corresponding author.

[5-7]. Results from these geophysical techniques are often presented in diverse ways including chloropleth, density, contour maps, profiles and pseudosections. Traditionally these geophysical data are processed to obtain depth profiles in 2D using various softwares. In this study we explore extending these traditional interpretation techniques to compute the continuity of the mineralized body at depth and develop a 3D model in a GIS environment, of the ore-bearing trends. This final 3D product, built up progressively from combined GIS softwares, is capable of displaying the inferred shape, structure and nature of the mineralized body as it varies with depth and will be useful to better appreciate and understand the nature and extent of the ore body over a wide area.

2. Location and Geology

The Belikombone hill gold prospect (14°00' - 14°25'E, 5°25' - 6°00'N) is a hydrothermal vein system and it is situated within the Lom Basin (Figure 1). The Lom Basin is a syn-depositional Neoproterozoic pull apart basin [8] bordered by strike-slip faults known locally as the Sanaga Fault (SF). The SF is a relay of the Central Cam-

eroon Shear Zone (CCSZ) System [8-12] which is a continental scale transcurrent fault and potentially a deep tapping crustal fault that has focused gold-bearing fluids into structures in the Lom Basin [13]. The Lom basin is composed mainly of metasedimentary rocks, grouped into two main structural and metamorphic units. These units include a monocyclic unit which comprises of Lom volcanoclastic series, orthogneiss, Mari quartzite and polygenic conglomerate [14] metamorphosed under green schist facies and associated with grabens. A polycyclic unit consisting of staurolite micaschists, Lom bridge gneisses, and staurolite-chloritoid mylonites, closely related to horst structures [8]. The mylonites are the main identifying features for the presence of the SF [14].

These units are intruded by quartz veins and granitoids (granite, monzonite and lamprophres) which show evidence of sinistral deformation [8]. Structurally the schist is well foliated with a general N70°E orientation, related to the shear zone system. Specifically, the Belikombone hill prospect is predominantly composed of mica schist and quartzites intruded by gold-bearing quartz veins that vary in size from a few centimeters to 10 m wide within artisanal gold pits and have a general NE-SW orientation

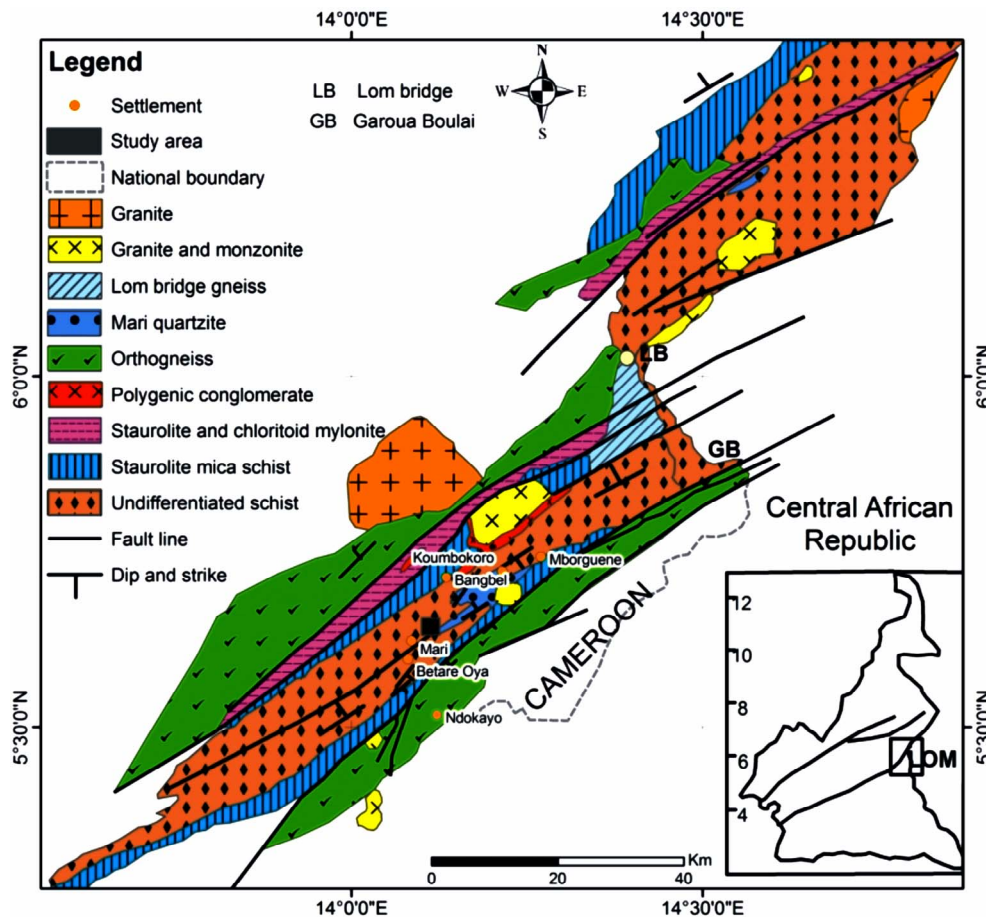


Figure 1. Location and geologic map of Betare Oya modified from [8,10].

and dips of 45° - 55° SE. The quartz veins show variable textures (ranging from hard massive and whitish quartz at surface to progressively brecciated, sheared, vuggy, sugary and brown to smoky quartz veins with iron oxide staining). This pervasive variation in quartz vein textures is associated to the different generations and recrystallization events commonly exhibited by quartz crystals. Hand specimen samples for some of these quartz veins show visible gold associated with disseminated sulphides and oxides. The quartzite show well preserved primary sedimentary structures such as current marks, indicating the flow direction, together with oblique cross stratification, and load casts.

3. Methods

The Belikombone hill prospect was selected for this study because of its gold potential that has been uncovered through structural and soil geochemical surveys from previous field campaigns. In the present study the IP (Induce polarization)—chargeability and resistivity surveys were carried out simultaneously along the same grid as the previous soil geochemical survey. A Syscal

Junior 48 resistivity meter was used to measure both the resistivity and chargeability of subsurface materials over the Belikombone hill gold prospect. The Schlumberger configuration array was used [15,16]. Vertical electrical soundings (VES) and horizontal profiling methods were adopted to obtain apparent resistivity and IP-chargeability data for 17 lines (**Figure 2**).

Measurements were done at fixed stations while systematically varying the electrode spacing, giving an approximate maximum penetration depth of 130 m. A total of 10 km (17 lines) of IP lines were completed at $50\text{ m} \times 50\text{ m}$ intervals for both the survey positions and the line spacing.

The IP-chargeability and resistivity data were generated and recorded automatically by the resistivity meter. These data were later extracted and processed using WINSEV 5, RED2INV softwares to convert the apparent resistivity data to true resistivity by inversion. The resistivity meter measures apparent resistivity from which pseudosections were developed and subsequently inverted to true resistivity 2D sections (**Figures 3(a)-(f)**).

The surface elevations are included in the final model, accounting for variations in measurement geometry due

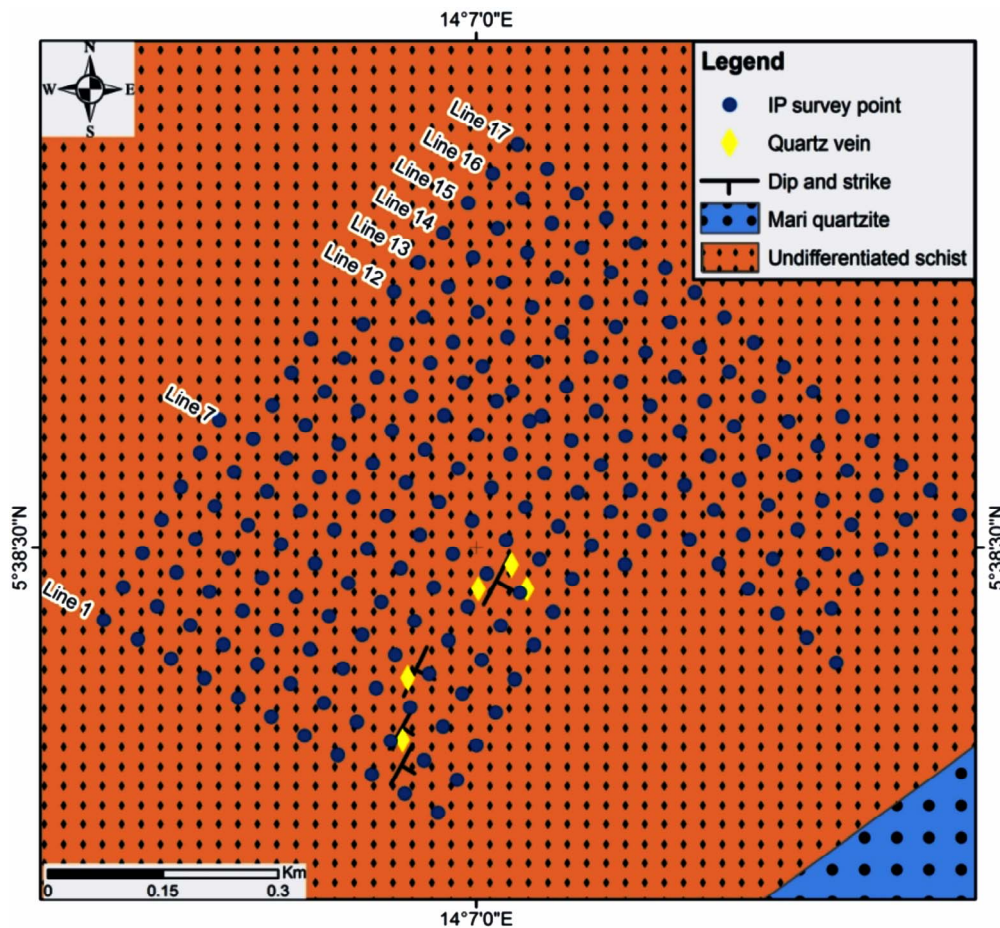


Figure 2. Resistivity and IP-chargeability survey grid ($50\text{ m} \times 50\text{ m}$) designed for the Belikombone hill gold prospect.

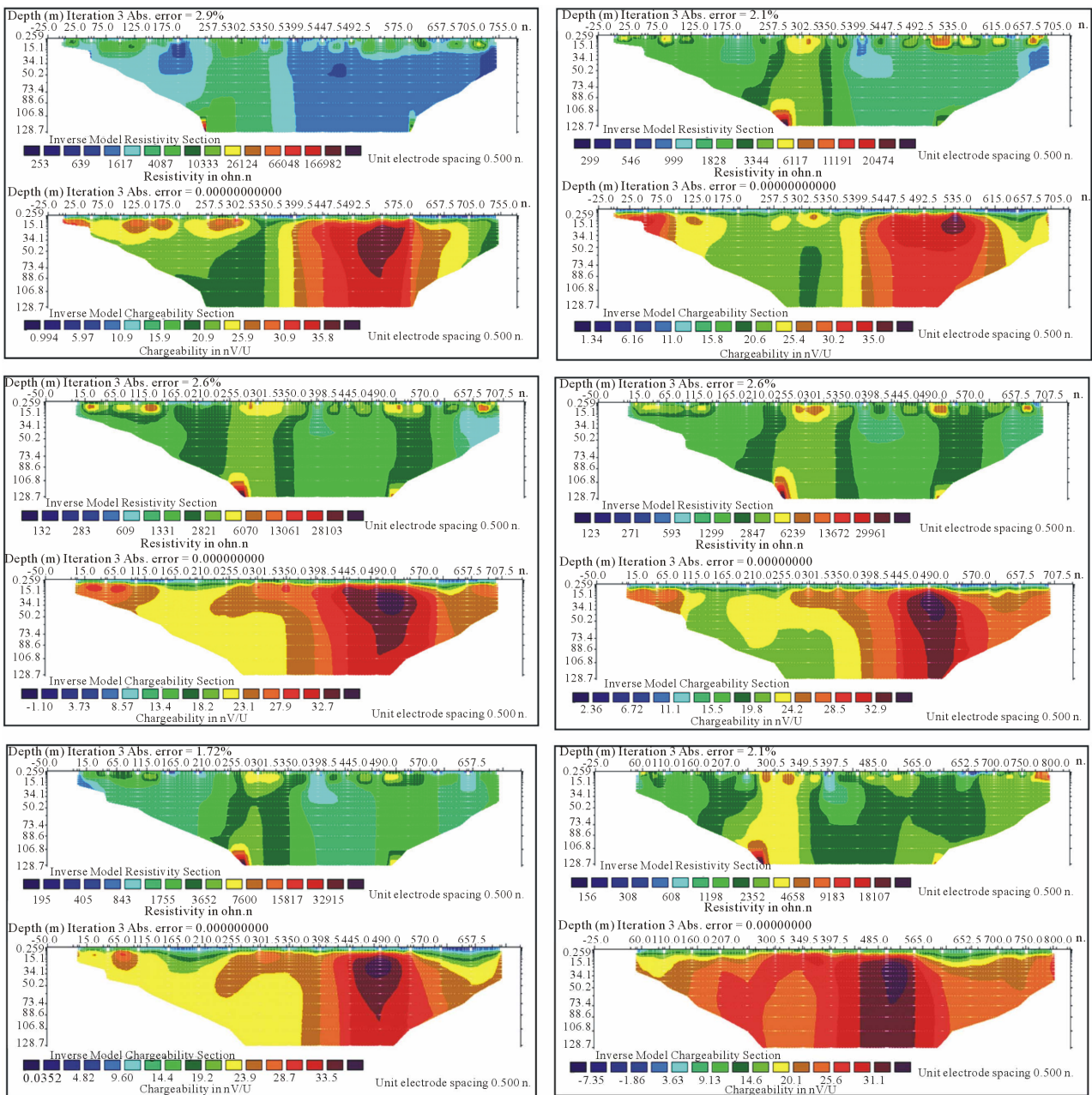


Figure 3. Inverted 2D sections for resistivity and IP-chargeability for six lines (12 to 17, Figure 2) obtained from VES data using Schlumberger configuration over the Belikombone hill gold prospect a: for line 12; b: 13; c: 14; d: 15; e: 16; f: 17. Anomalous zones for both resistivity and IP are represented by the deep-red to purple colouration on these sections.

to changing topography.

2D sections of the resistivity and IP-chargeability for each line were developed to a maximum depth of 130 m from the extracted data set.

3D contour maps and chloropleth maps of both resistivity and IP-chargeability were developed using SURFER 9.0. for depths of 1.9 m, 3.8 m, 5.7 m, 9.5 m, 19 m, 28.5 m, 38 , 57 m, 76 m and 95 m (Figures 4(a)-(j) and Figure 5(a)-(j)). These 3D IP maps were further stacked together to portray the nature of the mineralized body at depth.

4. Results and Synopsis

The geophysical data analyzed revealed a significant resistivity (Figures 4 and 6) and IP-chargeability (Figures 5 and 7) anomalies. Individual chargeability values within these anomalies range from 15 mV/V to 35 mV/V. These anomalies occur within zones of elevated resistivity that may represent silicification and quartz veining. This is confirmed by the location of quartz veins on areas with very high resistivity values as observed in Figures 4 and 6.

A. N. FON ET AL.

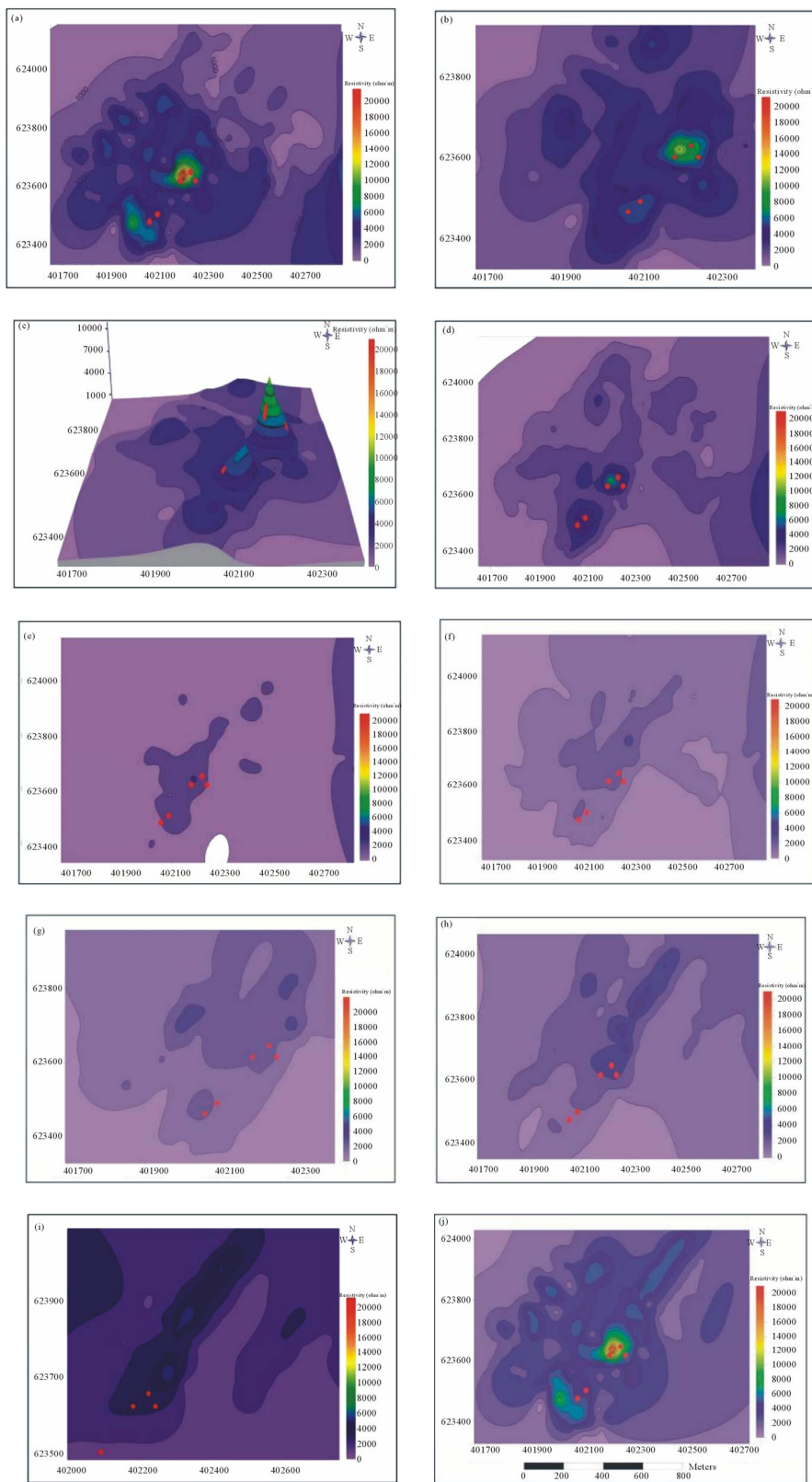


Figure 4. Resistivity contour maps derived for different depths at the Belikombone hill gold prospect. a: map for depth of 1.9 m; b: 3.8 m; c: 5.7 m; d: 9.5 m; e: 19 m; f: 28.5 m; g: 38 m; h: 57 m; i: 76 m and j: 95 m. Red dots on the map indicate location of quartz veins observed in artisanal pits and trenches. Zones of high resistivity anomalies are represented by the green to red colouration. All other colours are zones of low resistivity anomalies.

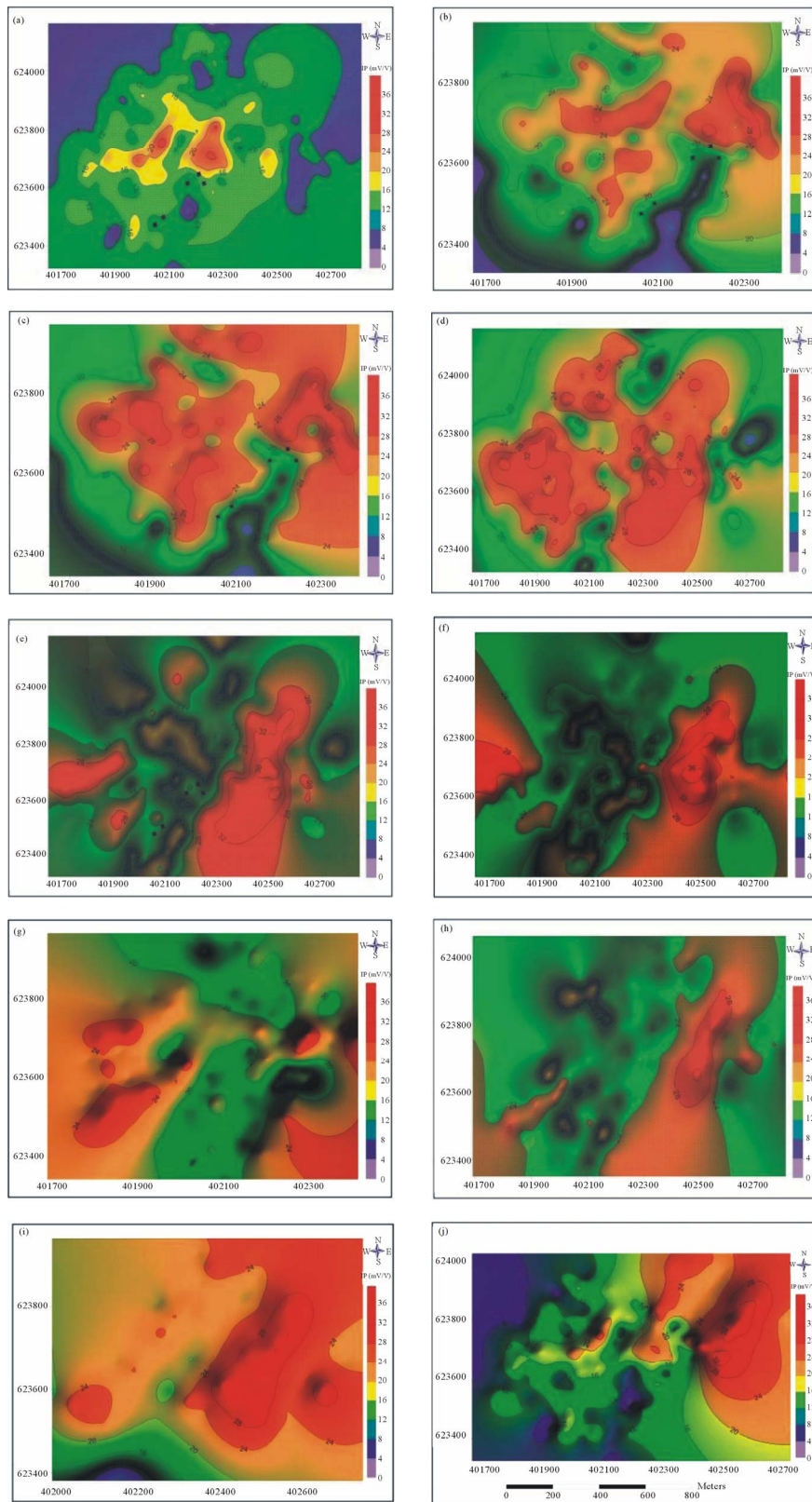


Figure 5. IP-chargeability contour maps for different depths at the Belikombone hill gold prospect. **a:** map for depths of 1.9 m, **b:** 3.8; **c:** 5.7m; **d:** 9.5; **e:** 19 m; **f:** 28.5, **g:** 38 m, **h:** 57 m, **i:** 76 m and **j:** 95 m. Black dots on the map indicate the location of quartz veins in artisanal pits and trenches. Zones of high IP anomalies are highlighted by red colouration. All other colours are zones of low IP anomalies.

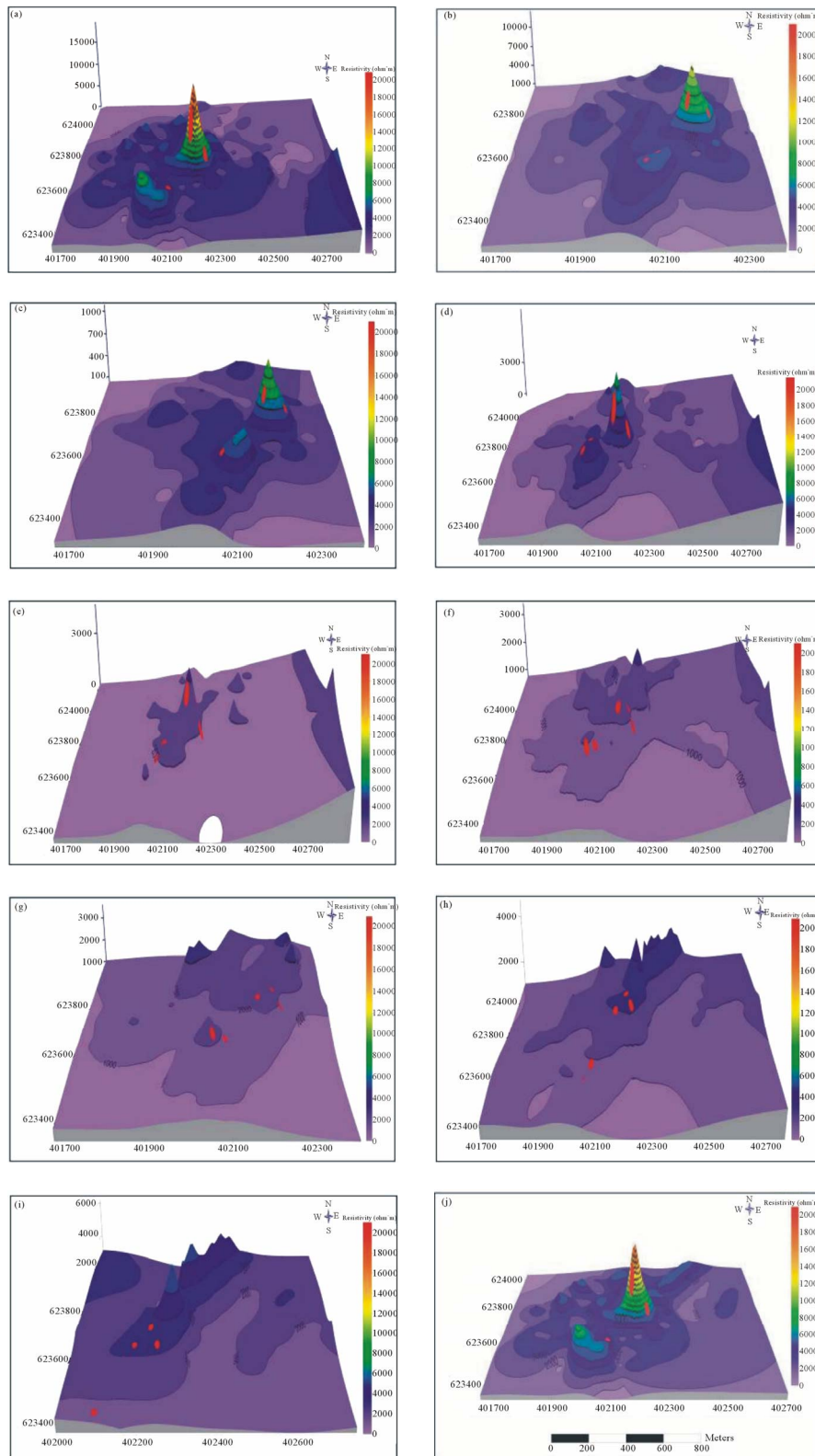


Figure 6. 3D resistivity maps for different depths at the Belikombone hill prospect. a: map for depths of 1.9 m, b: 3.8 m; c: 5.7 m; d: 9.5 m; e: 19 m; f: 28.5 m; g: 38 m; h: 57 m; i: 76 m and j: 95 m. Red dots on the map indicate the location of quartz veins in artisanal pits and trenches. Anomalous resistivity values are represented by green to red colouration at each depth these high resistivity values represent quartz veins. Variation in the shape of the resistivity contour patterns with depth highlights the irregular nature of the quartz veins. Purple and blue colourations represent relatively low resistivity values.

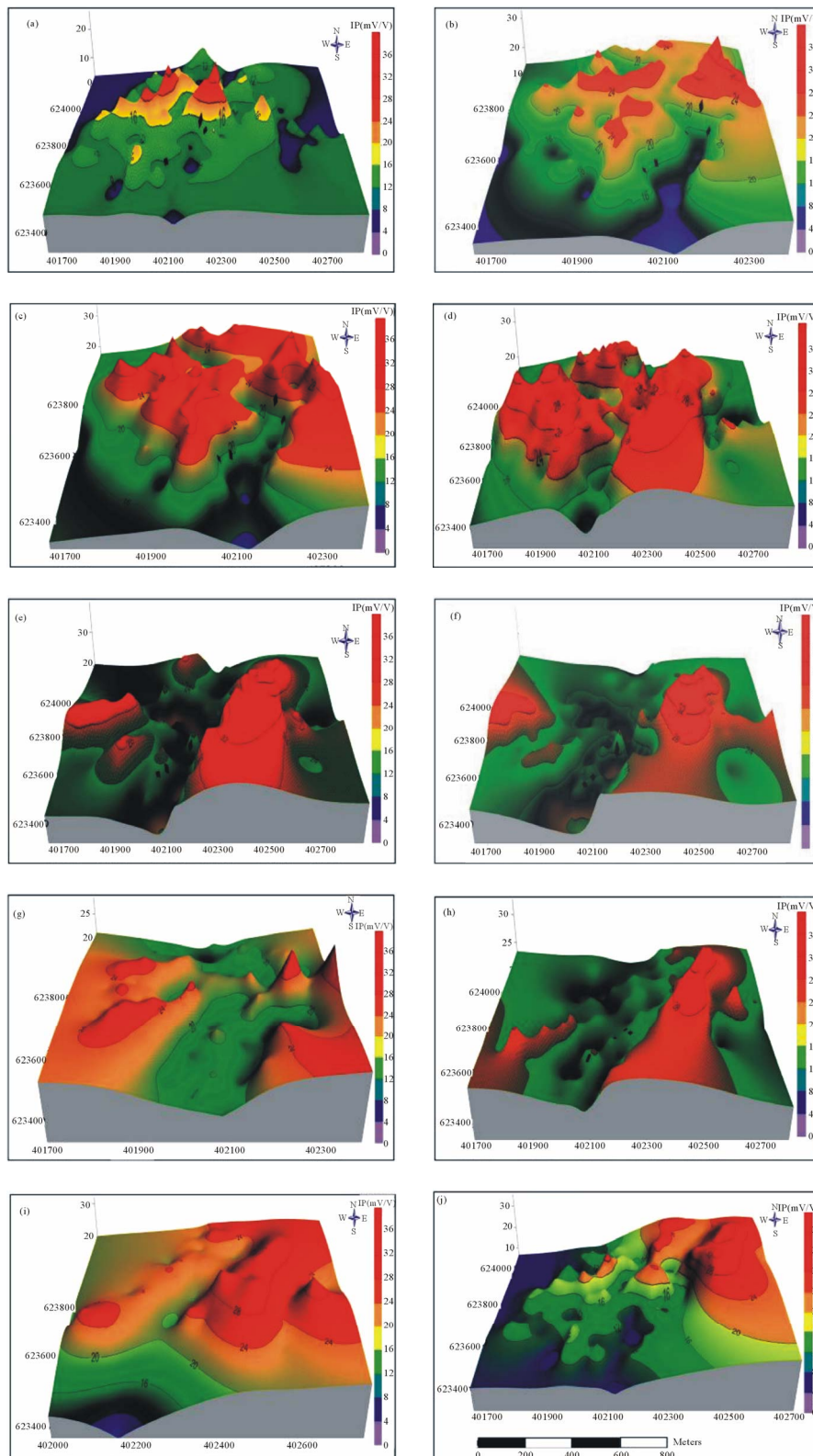


Figure 7. 3D IP chargeability maps for different depths at the Belikombone hill prospect. a: map for depths of 1.9 m, b: 3.8; c: 5,7 m; d: 9.5; e: 19 m; f: 28.5, g: 38 m, h: 57 m; i: 76 m and j: 95 m. Black dots on the map indicate the location of quartz veins. The anomalies defined by areas of high IP values (represented by the red colouration at each depth). The size and shape of the red patches varies with depth highlighting the irregular nature of the ore body. All other colours represent lower IP anomalies.

These high chargeability anomalies may represent disseminated sulphide \pm gold mineralization in the quartz veins. True resistivity and IP-chargeability sections were developed for 17 lines, each to a maximum depth of 130 m. Only sections for lines 12 to 17 have been presented here (**Figures 3(a)-(f)**) as examples.

It is observed that both the resistivity and IP sections show similar trends and consistent anomalies over zones of low resistivity and high chargeability (**Figures 3(a)-(f)**). Significantly high chargeability anomalies (>20 mV/V) are observed to the right of the 2D sections which correspond to relatively low resistivity (<1200 Ohm-m) anomalies (**Figures 3(a)-(f)**). Extremely high resistivity anomalies were observed for line 17 with values over $15000 \Omega\text{m}$. The almost homogeneous patterns and trends defined by the anomalous zones suggest that the mineralization is structurally controlled and follows a NE-SW orientation. This orientation is consistent with the local shear zone system in the Lom basin.

Contour maps of resistivity and IP-chargeability were computed for the total surface area concerned. The resistivity and IP-chargeability contour maps reveal distinct anomalous zones for the various depths (1.9 m, 3.8 m, 5.7 m, 9.5 m, 19 m, 28.5 m, 38 m, 57 m, 76 m and 95 m). To avoid ambiguity the general trends will be discussed rather than individual anomalies. The resistivity anomalies are very high and limited to a narrow surface area for depths of 1.9 m to 9.5 m, with values that range from $3000 \Omega\text{m}$ to over $15000 \Omega\text{m}$ (**Figures 4(a)-(d)**). Resistivity then decreases from 19 m to 57 m, (ranging from $1000 \Omega\text{m}$ to $3000 \Omega\text{m}$, **Figures 4(e)-(h)**) covering a wider surface area. It then rises again at 76 m to 95 m from $3000 \Omega\text{m}$ to over $15000 \Omega\text{m}$ (**Figures 4(i)** and **(j)**). Maximum resistivity values were recorded at two depths (1.9 m & 95 m). A distinct anomalous NE-SW trend is consistent at various depths. All the quartz veins located in artisanal pits and trenches fall on zones with high resistivity anomalies (**Figures 4(a)-(j)**). Thus quartz veins signatures are locally identified by high resistivity anomalies.

The IP anomalies are high and widespread at shallow depths from 1.9 m to 9.5 m, ranging from 20 mV/V to over 30 mV/V (**Figures 5(a)-(d)**). Optimum IP anomalies were recorded at 19 m and 28.5 m (**Figures 5(e)** and **(f)**) with values ranging from 20 mV/V to over 36 mV/V, a well distinct NE-SW trend is discernable. Relatively low IP was recorded at 38 m (**Figure 5(g)**) and it rises again at 57 m to 95 m with a similar NE-SW trend as above (**Figures 5(h)-(j)**). The high pervasive IP anomalies at shallow depths have no specific trend and may partly be related to prevalent clay minerals derived from the weathering and alteration of the micaschist as well as the massive sulphide-bearing quartz veins. The high IP anomalies at depth with well defined patterns are related

to the mineralized sulphide \pm goldbearing quartz veins that are sub-parallel to the regional shear system with a NE-SW orientation.

5. 3D Display of Resistivity and IP-Chargeability Maps

For better appraisal of the auriferous structures associated with the mineralized quartz vein, a 3D stacked model for IP-chargeability was developed for the various depths. Similar trends and anomalies observed for the contour maps above were consistent, though, now, with elevated peaks for easy and better visualisation (**Figures 6** and **7**).

The resistivity and chargeability 3D maps were compared to delineate the mineralized body. Furthermore, due to the significance of IP in relation to gold \pm sulphide mineralization, the 3D IP maps were combined and stacked together vertically according to their respective depths (**Figure 8**). A composite 3D IP map was developed from which the mineralized structure and ore body could be discerned down to a maximum depth of 95 m. This final product and a model of the inferred ore body is a function of the vertical variation of IP-chargeability and resistivity over a defined area.

6. Discussion and Conclusions

Ground geophysical surveys of IP/chargeability and resistivity are routinely used for a wide range of applications, ranging from environmental pollution studies (e.g. oil spills), lithology variation, hydrology in locating aquifers [17,18] to mineral exploration. However the effectiveness of these geophysical techniques in exploration are enhanced when integrated with geochemical and geological data [19] which define the target of investigation. Thus to enhance effective target recognition the element whose physical signature is investigated must be known. In this study, gold hosted by sulphide-bearing quartz veins within schist was the target of interest and the IP and resistivity were therefore efficient techniques in identifying the mineralized body.

Hydrothermal fluids that result in mineralization often cause changes in the adjacent rocks, a phenomenon often referred to as wall rock alteration [1,20]. These changes may be in the form of mineralogy (formation of neo-minerals, notably silica, sulphides and oxides) which in turn brings about extensive variation in physical properties of subsurface materials and they consequently exhibit variable geophysical signatures [21]. The contrast of these physical properties in rocks is revealed by the significant low resistivity and high IP-chargeability anomalies in altered wall rocks, relative to the non-mineralized and unaltered counterpart. It has been reported that the production of certain clay minerals by hydrothermal alteration significantly increases the electrical

conductivity of the rock [22] and thus might be an indication of mineralization. [21] suggested that epithermal gold deposits are produced by permeating hydrothermal fluids which are rich in ions, capable of reacting with the rocks over which they pass resulting in extensive alteration, and/or complete recrystallization. This is also applicable to mesothermal orogenic gold deposits where the deposits usually vary in their form, structures, size and physico-chemical environment, which makes their investigation obscure. Nevertheless employing ground

geophysical techniques of resistivity and IP has unraveled some of these concealed properties of subsurface mineralization in the Belikombene hill gold prospect.

From this study the 3D body varies in shape due to the heterogeneous nature of gold distribution or mineralization within the inferred ore body at different depths. The high resistivity at shallow depths reflects the late quartz generation resulting in barren and massive quartz veins. Resistivity variations with depth also reflect changes in quartz vein textures and crystallization regime

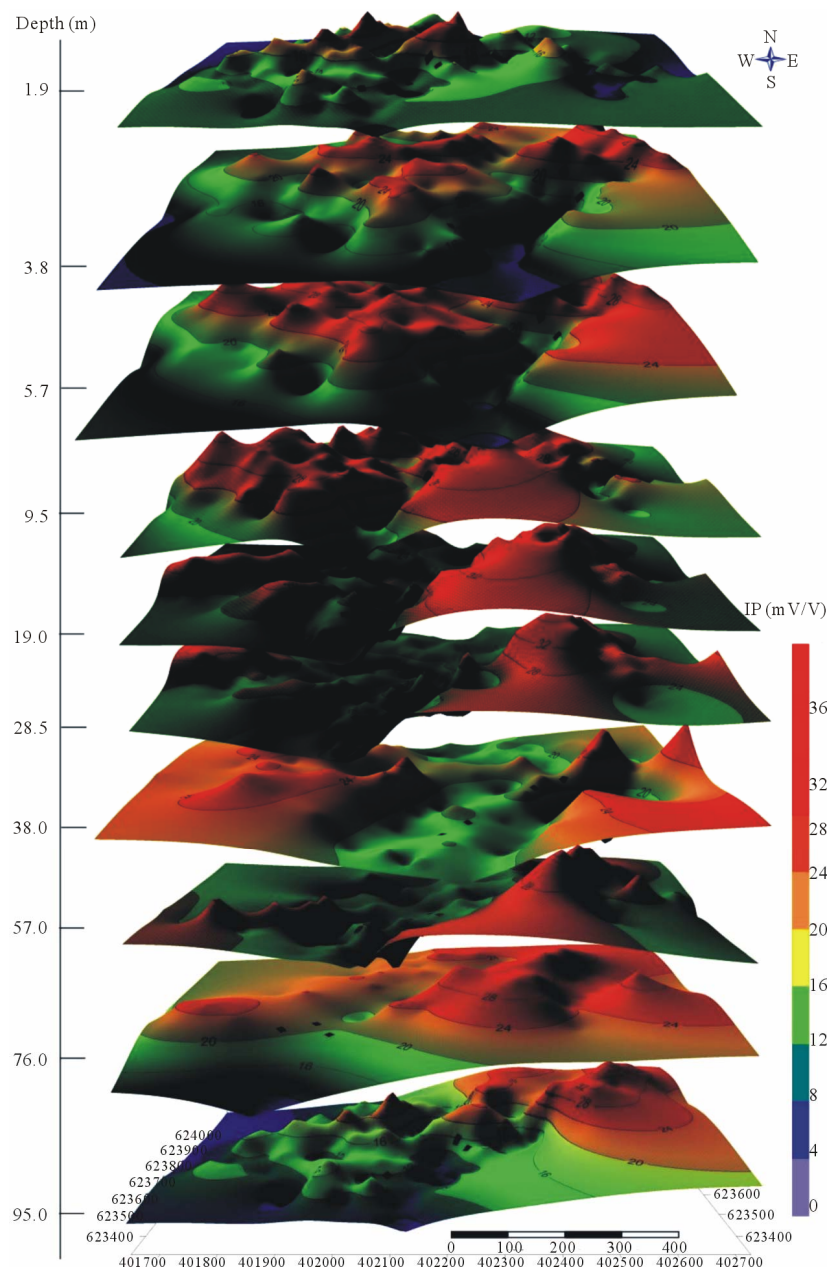


Figure 8. 3D composite IP-chargeability map for the Belikombene hill gold prospect displaying the variation in IP-chargeability with depth. The inferred ore body is defined by areas of high IP values (represented by the red colouration at each depth). The location of these red patches varies with depth highlighting the irregular nature of the ore body. All other colours are considered less prospective zone for gold.

with depth. Since the resistivity survey markedly identified potential quartz veins its 3D and contour maps represent the actual nature and extent of the quartz veins. The IP-chargeability variations indicate the extent and strength of mineralization (gold \pm sulphide concentration in the various materials). The high resistivity could partly be attributed to a fault sub-parallel to the regional structure with a NE-SW orientation.

The mineralized halo observed on the maps is estimated to be ca 300 - 400 m wide. This, therefore, suggests that not only the quartz veins are mineralized but also the altered adjacent wall rock to a lesser extent. However, [19] suggested that pervasive clay minerals associated with argillic-propylitic zones cause low-resistivity anomalies which are related to the reaction of the rocks with acid, steam-heated waters. In addition, the precipitation of quartz and adularia which commonly accompanies gold-silver mineralization causes an increase in resistivity with values locally exceeding 1000 Ω m [19]. The high resistivity observed in this study is therefore attributed to the presence of quartz veins, the relatively low resistivity areas correlate with high chargeability zones which are indicative of sulphides associated with the auriferous quartz veins and disseminated in the wall rock. The significant correlation of the Au-in-soil geochemical anomalies in the Belikombone hill gold prospect (from previous works) with the IP-chargeability and resistivity anomalies identified in this study, together with the consistent NE-SW trend associated with all the anomalies suggest a unique structural and mineralized body. These anomalies are therefore succinct drill targets for subsequent exploration and research works.

7. Acknowledgements

This article is part of a Ph.D. thesis by ANF at the University of Buea within a framework of cooperation with the Cameroon Mining Company (CAMINCO SA) initiated in 2006 with CES as the project academic coordinator. This contribution is within the research framework of "The Precambrian Mineral Belt of Cameroon" in the economic geology unit of University of Buea with other participating institutions. The authors express appreciation to the anonymous reviewers whose comments improved on the nature of the figures.

REFERENCES

- [1] C. E. Suh, "Sulphide Microchemistry and Hydrothermal Fluid Evolution in Quartz Veins, Batouri Gold District (Southeast Cameroon)," *Journal of the Cameroon Academy of Science*, Vol. 8, 2008, pp. 19-30.
- [2] P. E. J. Pitfield and S. D. G. Campbell, "Significance for Gold Exploration of Structural Styles of Auriferous Deposits in the Archaean Bulawayo-Bubi Greenstone Belt of Zimbabwe," *Transactions of the Institution of Mining and Metallurgy. Section B Applied Earth Science*, Vol. 105, 1996, pp. B41-B52.
- [3] T. G. Blenkinsop, S. D. G. Campbell, P. E. J. Pitfield and T. Muzondo, "Contrasting Structural Controls on Gold Mineralization along the Eldorado Shear Zone, Zimbabwe," *Transactions of the Institution of Mining and Metallurgy. Section B, Applied Earth Science*, Vol. 105, 1996, pp. B53-B59.
- [4] R. J. Bowell, E. O. Afreh, N. d'A. Laffoley, E. Hanssen, S. Abe, R. K. Yao and D. Pohl, "Geochemical Exploration for Gold in Tropical Soils: Four Contrasting Case Studies from West Africa," *Transactions of the Institution of Mining and Metallurgy. Section B: Applied Earth Science*, Vol. 105, 1996, pp. B12-B33.
- [5] H. Hase, T. Hashimoto, S. Sakanaka, W. Kanda and Y. Tanaka, "Hydrothermal System Beneath Aso Volcano as Inferred from Self Potential Mapping and Resistivity Structure," *Journal of Volcanology and Geothermal Research*, Vol. 134, No. 4, 2005, pp. 259-278.
[doi:10.1016/j.jvolgeores.2004.12.005](https://doi.org/10.1016/j.jvolgeores.2004.12.005)
- [6] F. Cella, M. Fedi, G. Florio, M. Grimaldi and A. Rapolla, "Shallow Structure of the Somma-Vesuvius Volcano from 3D Inversion of Gravity Data," *Journal of Volcanology and Geothermal Research*, Vol. 161, No. 4, 2007, pp. 303-317. [doi:10.1016/j.jvolgeores.2006.12.013](https://doi.org/10.1016/j.jvolgeores.2006.12.013)
- [7] I. Caglar and T. Isseven, "Two Dimensional Geoelectrical Structure of the Goynok Geothermal Area Northwest Anatolia, Turkey," *Journal of Volcanology and Geothermal Research*, Vol. 134, No. 3, 2004, pp. 183-198.
[doi:10.1016/j.jvolgeores.2004.01.003](https://doi.org/10.1016/j.jvolgeores.2004.01.003)
- [8] V. Ngako, P. Affaton, J. M. Nnange and Th. Njanko, "Pan African Tectonic Evolution on Central and Southern Cameroon: Transpression and Transtension during Sinistral Shear Movements," *Journal of African Earth Sciences*, Vol. 36, No. 3, 2003, pp. 207-214.
[doi:10.1016/S0899-5362\(03\)00023-X](https://doi.org/10.1016/S0899-5362(03)00023-X)
- [9] S. F. Toteu, W. R. Van Schmus, J. Penaye and A. Michard, "New U-Pb and Sm-Nd Data from North-Central Cameroon and Its Bearing on the Pre-Pan-African History of Central Africa," *Precambrian Research*, Vol. 108, No. 1-2, 2001, pp. 45-73.
[doi:10.1016/S0301-9268\(00\)00149-2](https://doi.org/10.1016/S0301-9268(00)00149-2)
- [10] S. F. Toteu, J. Penaye, E. Deloule, W. R. Van Schmus and R. Tchameni, "Diachronous Evolution of Volcano-Sedimentary Basins North of the Congo Craton: Insights from U-Pb Ion Microprobe Dating of Zircons from the Poli, Lom and Yaoundé Groups (Cameroon)," *Journal of African Earth Sciences*, Vol. 44, 2006, pp. 428-442.
[doi:10.1016/j.jafrearsci.2005.11.011](https://doi.org/10.1016/j.jafrearsci.2005.11.011)
- [11] B. Kankeu, O. Greiling and Z. J. P. Nzenti, "Pan African Strike Slip Tectonic in Eastern Cameroon Magnetic Fabrics (AMS) and Structures in the Lom Basin and Its Gneissic Basement," *Precambrian Research*, Vol. 174, 2009, pp. 258-272. [doi:10.1016/j.precamres.2009.08.001](https://doi.org/10.1016/j.precamres.2009.08.001)
- [12] B. Kankeu, R. O. Greiling, J. P. Nzenti, J. Bassahak and J. V. Hell, "Strain Partitioning along the Neoproterozoic Central African Shear Zone System: Structures and Magnetic Fabrics (AMS) from the Meiganga Area, Cameroon," *Neues Jahrbuch für Geologie und Paläontologie*

Abhandlungen, Vol. 265, 2012, pp. 27-47.

- [13] A. Dane, "Lom River Property: Geological Report," Bridge Consulting, 1998, p. 86.
- [14] D. Soba, "La Série de Lom: Étude Géologique et Géochronologique du Bassin Volcano-Sédimentaire de la Chaîne Panafricaine à l'Est du Cameroun," Thèse de doctoral d'Etat, Université Pierre et Marie Curie, Paris, 1989.
- [15] C. Schlumberger, "Étude Sur la Prospection Électrique du Sous-Sol," Gauthier, Villars, 1920.
- [16] J. S. Sumner, "Principle of Induced Polarization for Geophysical Exploration," Elsevier Scientific, Amsterdam, 1978.
- [17] W. A. Teikeu, T. Ndougsa-Mbarga, P. N. Njandjock, T. C. Tabod, "Geoelectric Investigation for Groundwater Exploration in Yaounde Area, Cameroon," *International Journal of Geosciences*, Vol. 3, No. 3, 2012, pp. 640-649. [doi:10.4236/ijg.2012.33064](https://doi.org/10.4236/ijg.2012.33064)
- [18] A. S. Al Dulaymi, E. A. R. Al-Heety and B. M. Hussien, "Geo-Electrical Investigation of Mullusi Aquifer, Rutba, Iraq," *International Journal of Geosciences*, Vol. 3, No. 3, 2012, pp. 549-564. [doi:10.4236/ijg.2012.33056](https://doi.org/10.4236/ijg.2012.33056)
- [19] R. G. Allis, "Geophysical Anomalies over Epithermal Systems," *Journal of Geochemical Exploration*, Vol. 36, 1990, pp. 339-374. [doi:10.1016/0375-6742\(90\)90060-N](https://doi.org/10.1016/0375-6742(90)90060-N)
- [20] R. C. Henneberger and P. R. L. Browne, "Hydrothermal Alteration and Evolution of the Ohakuri Hydrothermal System, Taupo Volcanic Zone, New Zealand," *Journal of Volcanology and Geothermal Research*, Vol. 34, No. 3-4, 1988, pp. 211-231. [doi:10.1016/0377-0273\(88\)90034-0](https://doi.org/10.1016/0377-0273(88)90034-0)
- [21] R. J. Irvine and M. J. Smith, "Geophysical Exploration for Epithermal Gold Deposits," *Journal of Geochemical Exploration*, Vol. 36, No. 1-3, 1990, pp. 375-412. [doi:10.1016/0375-6742\(90\)90061-E](https://doi.org/10.1016/0375-6742(90)90061-E)
- [22] P. H. Nelson and L. A. Anderson, "Physical Properties of Ash Flow Tuff from Yucca Mountains Nevada," *Journal of Geophysical Research*, Vol. 97, No. B5, 1992, pp. 6823-6841. [doi:10.1029/92JB00350](https://doi.org/10.1029/92JB00350)